JAASCI
http://jaasci.com
JOURNAL OF ADVANCED APPLIED SCIENCES
e-ISSN: 2979-9759
PRENSIP
https://prensip.gen.tr

RESEARCH ARTICLE

Influence of Blast Furnace Slag Content on the Density, Microstructure, Hardness, and Wear Behavior of Pure Aluminum Matrix Composites Fabricated by Powder Metallurgy

Hakan Ada[1,2]✉ • Sadiye Yazır[2]

[1]Gazi University, Faculty of Technology, Department of Metallurgical and Materials Engineering, Ankara/Türkiye
[2]Kastamonu University, Faculty of Engineering and Architecture, Department of Mechanical Engineering, Kastamonu/Türkiye

ARTICLE INFO

Article History
Received: 09.06.2026
Accepted: 19.06.2026
First Published: 28.06.2026

Keywords
Aluminum matrix composites
Blast furnace slag (BFS)
Hardness
Microstructure
Powder metallurgy
Wear behavior

ABSTRACT

This study investigates the effects of blast furnace slag (BFS) reinforcement on the microstructural, physical, mechanical, and tribological properties of pure aluminum matrix composites. Composite samples containing 0.125, 0.25, 0.5, 1, 2, 4, 8, 12, and 16 wt.% BFS were fabricated by powder metallurgy. Theoretical and experimental densities were determined, relative density and porosity values were calculated, and the samples were characterized using optical microscopy, hardness measurements, and pin-on-disk wear tests. The results showed that the addition of BFS had a limited influence on the theoretical density due to the similar densities of aluminum and BFS. However, experimental and relative density values decreased at higher reinforcement levels, while porosity increased noticeably. Although all composites exhibited relative densities above 95%, increasing BFS content adversely affected densification behavior. Optical microscopy revealed a relatively homogeneous microstructure at BFS contents of 2–4 wt.%, whereas particle agglomeration and pore formation became more pronounced at higher reinforcement levels. Hardness results indicated that the effect of BFS reinforcement was not linear. Hardness values remained comparable to those of unreinforced aluminum at BFS contents of 2–4 wt.% but decreased significantly at higher reinforcement levels due to increased porosity and particle agglomeration. A similar trend was observed in the wear tests. The unreinforced aluminum sample exhibited the lowest weight loss, while wear loss increased with increasing BFS content. In particular, composites containing 8–16 wt.% BFS showed considerably higher weight loss, which was associated with increased porosity, microstructural heterogeneity, and reduced hardness. The findings demonstrate that blast furnace slag can be used as a low-cost, environmentally friendly reinforcement material in aluminum matrix composites. However, excessive BFS additions promote porosity and agglomeration, which adversely affect densification, hardness, and wear performance. Considering the combined results of density, microstructure, hardness, and wear behavior, BFS contents of 2–4 wt.% provided the most balanced overall performance among the investigated composites.

Please cite this paper as follows:
Ada, H., & Yazır, S. (2026). Influence of blast furnace slag content on the density, microstructure, hardness, and wear behavior of pure aluminum matrix composites fabricated by powder metallurgy. *Journal of Advanced Applied Sciences*, *5*(1), 34-44. https://doi.org/10.61326/jaasci.v5i1.501

1. Introduction

Powder metallurgy (PM) is an advanced manufacturing technique that enables the production of components with simple or complex geometries while maintaining dimensional accuracy and tight tolerances. Owing to its relatively low energy consumption, reduced material waste, and cost-effectiveness, PM has become one of the most widely adopted processing routes for fabricating metal matrix composites (MMCs). In recent years, PM-produced ceramic-reinforced composites have demonstrated significant advantages over

✉ Correspondence
E-mail address: hakanada@gazi.edu.tr

conventionally cast materials, particularly in microstructural control and mechanical performance (Chintada et al., 2022; Kok, 2005; Nayak et al., 2022; Usca et al., 2021). Consequently, numerous composite components employed in aerospace, automotive, defense, and electronics industries are currently manufactured using PM techniques (Kumar et al., 2011). Furthermore, the rapid development of additive manufacturing technologies has further increased the importance of powder-based processing methods in modern manufacturing systems (Gräbner et al., 2022).

Metal matrix composites fabricated by PM generally exhibit lower densities and higher hardness values than their cast counterparts. However, residual porosity is a characteristic feature of the PM process. Despite this limitation, PM offers a significant advantage by facilitating a more homogeneous distribution of reinforcement particles within the matrix (Abdizadeh et al., 2014). In conventional casting methods, reinforcement particles often agglomerate and settle, leading to local variations in physical and mechanical properties. In particular, the agglomeration of ceramic particles in cast aluminum matrix composites may weaken matrix–reinforcement interfacial bonding and adversely affect the composite's overall mechanical performance (Chen & Zhang, 1993).

Aluminum and its alloys are among the most widely used matrix materials for MMCs because of their low density, high specific strength, excellent corrosion resistance, good ductility, and economic availability. Nevertheless, the relatively poor hardness and wear resistance of aluminum limit its use in demanding engineering applications. To overcome these shortcomings, various ceramic reinforcements have been incorporated into aluminum matrices. Silicon carbide (SiC) and alumina (Al_2O_3) are among the most commonly employed reinforcements owing to their high elastic modulus, excellent high-temperature stability, superior strength, and thermal shock resistance (Hull, 1998; Şap et al., 2021a; Şap et al., 2021b; Usca et al., 2022). In addition, their ability to form strong interfacial bonds with aluminum and provide enhanced wear resistance significantly improves the mechanical and tribological properties of aluminum-based composites.

Blast furnace slag (BFS) is an industrial by-product generated during iron production in blast furnaces and consists primarily of CaO, SiO_2, and Al_2O_3 compounds (Dorum et al., 2009; Erdoğdu & Kurbetçi, 2003; Tokyay & Erdoğdu, 2002; Yalçın & Gürü, 2006). Its chemical composition and crystalline structure largely govern the performance of BFS. Depending on the cooling conditions, BFS may exhibit different microstructural characteristics. Rapid cooling of molten slag produces granulated blast furnace slag with a predominantly amorphous (glassy) structure, which exhibits pozzolanic activity when finely ground (Bilim & Atiş, 2011; Erdoğan, 1995). Owing to these characteristics, BFS has been widely used in the construction industry for decades as an additive that improves strength, durability, and long-term service performance (Babu & Kumar, 2000; Douglas & Brvestetr, 1990; Malolepszy & Petri, 1986; Özkan, 2007; Shi & Day, 1992).

The high contents of SiO_2, Al_2O_3, and CaO make BFS a promising low-cost and environmentally friendly ceramic-based reinforcement material. With the growing emphasis on sustainable manufacturing, the utilization of industrial waste products as reinforcements in MMCs has attracted considerable attention from both economic and environmental perspectives. Nevertheless, studies concerning the use of BFS as a reinforcement material in metal matrix composites remain extremely limited. In particular, the effects of BFS on the microstructural evolution, densification behavior, hardness, and wear performance of aluminum matrix composites have not yet been comprehensively investigated.

Dorum et al. (2009) examined the physical, chemical, and mineralogical characteristics of ground granulated blast-furnace slag-blended cements and reported that BFS significantly influenced the hydration behavior and microstructural development. Similarly, Binici et al. (2016) demonstrated that incorporating BFS improved the wear resistance and impermeability of concrete. Saran (2007) reported that ground granulated blast-furnace slag enhanced the durability of concrete and contributed positively to corrosion resistance. These studies collectively indicate that BFS can serve as a performance-enhancing constituent in engineering materials.

Despite these promising findings, research focusing on BFS-reinforced metal matrix composites remains scarce. One of the few studies directly related to MMCs was conducted by Şanlı (2017), who employed Al6061 alloy as the matrix material and investigated the use of blast furnace slag alongside conventional ceramic reinforcements such as SiC and Al_2O_3. The composites were fabricated using a two-stage stir casting process, and their porosity, hardness, microstructure, and fatigue behavior were evaluated. The results revealed that BFS significantly improved hardness and enhanced fatigue strength up to certain reinforcement levels. However, BFS-reinforced composites exhibited higher porosity than composites reinforced with conventional SiC and Al_2O_3 particles. Furthermore, the study focused on an Al6061 alloy matrix, leaving the interaction between BFS and pure aluminum, as well as its influence on microstructural and mechanical properties, largely unexplored.

To the best of the authors' knowledge, studies investigating BFS as the sole reinforcement in pure aluminum matrix composites fabricated by powder metallurgy are not available in the open literature. In addition, the combined influence of BFS content on densification behavior, microstructural evolution, hardness, and wear performance has not been systematically evaluated. Therefore, a significant knowledge gap remains regarding the effectiveness of BFS as a sustainable reinforcement material for pure aluminum-based composites.

In addition, numerous studies have investigated the effects of ceramic reinforcements on aluminum matrix composites. Şenel (2020) produced aluminum matrix composites reinforced with varying amounts of B_4C and Al_2O_3 via powder metallurgy and reported significant increases in hardness and compressive strength with increasing reinforcement content. In particular, B_4C-reinforced composites exhibited a denser microstructure and superior mechanical performance. These findings confirm the effectiveness of ceramic reinforcements in enhancing the properties of aluminum-based composites.

Similarly, Özer et al. (2024) investigated the influence of different sintering techniques on the density, hardness, and wear behavior of Al-15Si-2.5Cu-0.5Mg/B_4C composites produced by powder metallurgy. The authors reported that porosity was critical to the mechanical and tribological performance of the composites and demonstrated that increased porosity adversely affected both hardness and wear resistance. Their findings highlighted the strong relationship between densification behavior, microstructural integrity, and wear performance in particle-reinforced aluminum matrix composites.

Based on the available literature, although blast furnace slag has been extensively used in construction materials, its application as a reinforcement in metal matrix composites has received limited attention. The microstructural modifications induced by BFS and their effects on the density, hardness, and wear behavior of aluminum matrix composites remain poorly understood. Moreover, most existing studies have focused on aluminum alloys rather than pure aluminum matrices.

Unlike the limited number of available studies that mainly employed aluminum alloys and casting-based production routes, the present work focuses on pure aluminum matrix composites produced by powder metallurgy and reinforced exclusively with varying BFS contents. This approach enables a systematic evaluation of the relationship between BFS addition, densification characteristics, microstructural development, hardness, and wear resistance.

Therefore, investigating the behavior of BFS in pure aluminum matrix composites is of both scientific and practical significance. In the present study, pure aluminum matrix composites with varying BFS contents were fabricated via powder metallurgy. The effects of BFS content on relative density, microstructure, hardness, and wear behavior were systematically investigated. The novelty of this study lies in the use of blast furnace slag, an industrial waste material, as a low-cost, environmentally sustainable reinforcement in pure aluminum matrix composites, and in the comprehensive assessment of its effects on both physical and tribological properties. Furthermore, the feasibility of using blast-furnace slag as a low-cost, sustainable reinforcement material for aluminum matrix composites was evaluated, and the optimal reinforcement level was determined.

2. Experimental Studies

2.1. Material

In this study, aluminum (Al) powder was used as the matrix material, and blast-furnace slag (BFS) was employed as the reinforcement for the fabrication of aluminum matrix composites. The Al powder used as the matrix material had a purity of 99.9%, a particle size smaller than 75 µm, and was supplied by Nanokar. The BFS used as the reinforcement material had a particle size smaller than 45 µm, a density of 2.80 g/cm³, and was obtained from Ereğli Iron and Steel Works (ERDEMİR). The chemical composition of the blast furnace slag used as the reinforcement material is presented in Table 1.

Table 1. Chemical composition of the BFS used as reinforcement material.

Compound	**SiO_2**	**Fe_2O_3**	**Al_2O_3**	**CaO**	**MgO**	**Na_2O**	**K_2O**	**SO_3**	**TiO_2**	**P_2O_5**
Wt. %	38.26	1.07	16.44	33.9	7.29	0.58	1.1	0.35	1.01	-

2.2. Fabrication of Composite Samples

Different reinforcement contents were selected to investigate the effect of blast furnace slag (BFS) on the properties of pure aluminum matrix composites over a wide composition range. Accordingly, composite samples containing 0.125, 0.25, 0.50, 1, 2, 4, 8, 12, and 16 wt.% BFS was prepared by powder metallurgy. The composition ratios of the fabricated Al–BFS composite samples are presented in Table 2.

The Al and BFS powders were weighed according to the predetermined compositions and mixed in a Retsch PM100 planetary ball mill at a rotational speed of 300 rpm for 90 min using a powder-to-ball weight ratio of 1:10. Following the mixing process, the powder mixtures were compacted into cylindrical specimens with a diameter of 10 mm and a height of 15 mm. Compaction was performed by uniaxial cold pressing under a pressure of 600 MPa.

The green compacts obtained after pressing were subsequently sintered at 600 °C for 90 min under an argon atmosphere. The processing parameters employed for the fabrication of the composite materials are summarized in Table 3.

Table 2. Composition ratios of the Al–BFS composite samples.

Specimens	Al %	BFS %
S0	100	-
S1	99.875	0.125
S2	99.750	0.250
S3	99.500	0.500
S4	99.000	1.000
S5	98.000	2.000
S6	96.000	4.000
S7	92.000	8.000
S8	88.000	12.000
S9	84.000	16.000

Table 3. Processing parameters used for the fabrication of Al–BFS composite samples.

Parameter	Value
Powder-to-ball ratio	1/10
Mixing speed	300 rpm
Mixing time	90 min
Compaction pressure	600 MPa
Sintering atmosphere	Argon atmosphere
Sintering temperature	600°C
Sintering time	90 min

Figure 1. Macroscopic appearance of the Al–BFS composite samples produced with different BFS reinforcement contents.

Figure 1 shows the macroscopic appearance of the Al–BFS composite samples produced using the processing parameters given in Table 3. Visual examination revealed no evidence of macroscopic defects, including cracks, fractures, or shape distortions, indicating that the selected powder metallurgy processing parameters were sufficient to produce sound composite specimens across the entire composition range.

2.3. Microstructural and Mechanical Characterization

Prior to microstructural and mechanical characterization, the fabricated composite samples were prepared in accordance with standard metallographic procedures. The samples were mounted using an APM Opal 460 mounting machine and subsequently ground on an APM Saphir 330 grinding and polishing system with SiC abrasive papers of grit sizes 120, 240, 400, 800, 1200, and 2500. Final polishing was performed using 6 µm and 3 µm monocrystalline diamond suspensions. To reveal the microstructure, the polished surfaces were etched using a reagent consisting of 5 mL HNO_3, 3 mL HCl, 2 mL HF, and 190 mL distilled water.

The theoretical densities of the Al–BFS composite samples were calculated using the rule of mixtures. In contrast, the experimental densities were determined using the liquid displacement method, in accordance with Archimedes' principle. Relative density and porosity values were subsequently calculated from the theoretical and experimental density results. The equations used to determine the theoretical density, experimental density, relative density, and porosity are presented in Eqs. (1)–(4), respectively.

$$\rho_T= [(\%w_m.\rho_m)+ (\%w_R.\rho_R)] \quad (1)$$

$$\rho_E=[m_D/(m_S-m_{SIW})]\rho_W \quad (2)$$

$$\rho_R=(\rho_E/\rho_T) \text{ x } 100 \quad (3)$$

$$\%P=[1 - (\rho_E/\rho_T)] \text{ x } 100 \quad (4)$$

In these equations, ρ_T, ρ_E, ρ_R, and P represent the theoretical density, experimental density, relative density, and porosity, respectively. The terms ρ_m and ρ_r denote the densities of the matrix and reinforcement materials, while w_m and w_r represent the weight fractions of the matrix and reinforcement, respectively. Furthermore, m_D, m_S, and m_{SIW} correspond to the dry mass, saturated mass, and suspended mass in water of the composite specimen, respectively, whereas ρ_W represents the density of water.

Microstructural examinations were carried out using a Leica DMI5000M optical microscope equipped with a Leica DFC 320 digital camera. Optical micrographs were obtained at a magnification of 100×.

The macrohardness values of the composite samples were determined using an Emcotest DuraVision 200 hardness tester. For each sample, measurements were taken from five different locations, and the average values were reported. Hardness tests were performed according to the Brinell method using a 2.5-mm-diameter ball indenter under an applied load of 31.25 kg.

The wear behavior of the composite samples was evaluated using a UTS T10/20 tribometer operating in a pin-on-disk configuration. A Hardox 450 steel disk with a diameter of 120 mm and a thickness of 10 mm was used as the counterface material. Wear tests were conducted under an applied load of 10 N, a sliding speed of 1 m/s, and a sliding distance of 1000 m.

3. Results and Discussion

The effects of blast furnace slag (BFS) reinforcement on the physical, microstructural, mechanical, and tribological properties of aluminum matrix composites were systematically investigated. Relative density, optical microscopy, hardness, and wear test results were analyzed to evaluate the influence of reinforcement content on composite performance. The experimental findings are presented and discussed in the following sections with reference to relevant literature.

3.1. Density Measurements

The theoretical and experimental densities of the Al–BFS composite samples were determined using Eqs. (1) and (2), respectively, and the corresponding results are presented in Figure 2. Based on these density values, the relative density and porosity of the composites were calculated according to Eqs. (3) and (4). The calculated relative density and porosity values are shown in Figure 3.

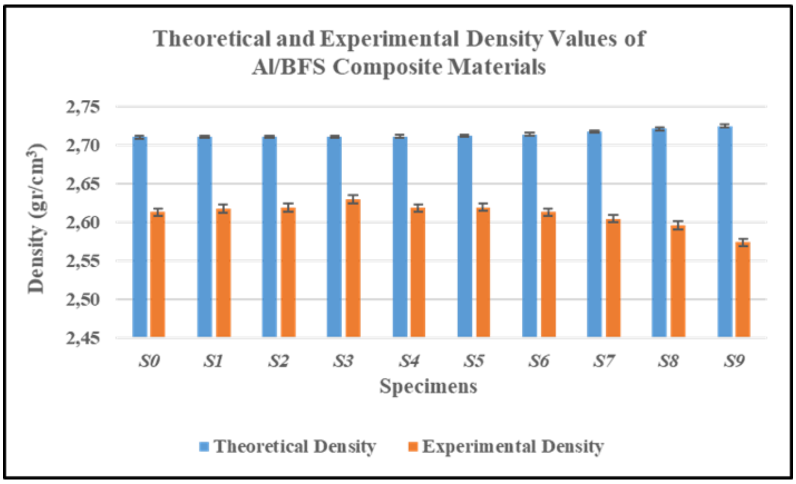

Figure 2. Variation of theoretical and experimental densities of Al–BFS composites as a function of BFS reinforcement content.

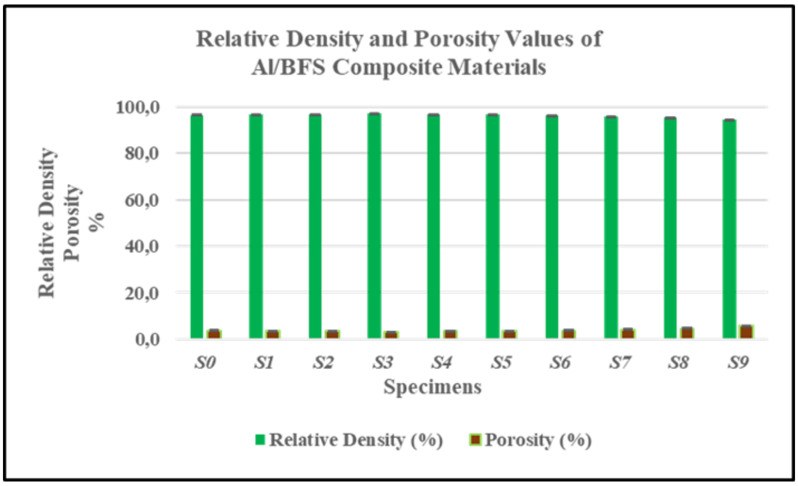

Figure 3. Relative density and porosity values of the Al–BFS composite samples.

Figure 2 shows the theoretical and experimental density values of the Al–BFS composites. As shown, the theoretical and experimental densities exhibited similar trends across the investigated composition range. Since the density of BFS (2.80 g/cm^3) is very close to that of the aluminum matrix (2.71 g/cm^3), increasing the BFS content resulted in only a slight increase in the theoretical density. Accordingly, the theoretical density values varied within a narrow range of approximately 2.71–2.73 g/cm^3 for all compositions.

Examination of the experimental density results revealed that the density values remained relatively close to the theoretical values at BFS contents of 2–4 wt.%. However, a noticeable decrease in experimental density was observed as the BFS content increased beyond this range. In particular, composites containing 8, 12, and 16 wt.% BFS exhibited lower experimental density values, indicating a deterioration in densification behavior as reinforcement content increased. This behavior can be attributed to intensified particle–particle interactions, the formation of interfacial voids between the aluminum matrix and BFS particles, and restricted diffusion during sintering. Consequently, higher BFS contents hindered effective particle bonding and reduced the overall densification efficiency of the composites.

Furthermore, the experimental density values were lower than the corresponding theoretical values for all compositions. This difference indicates residual porosity that could not be eliminated despite the compaction and sintering inherent to powder metallurgy. The increasing discrepancy between theoretical and experimental density values at higher BFS contents suggests increased porosity in the composite structure. These findings are consistent with the relative density, porosity, and optical microscopy results presented in the subsequent sections and indicate that increasing BFS content adversely affects densification and microstructural integrity.

The relative density and porosity values of the Al–BFS composites are presented in Figure 3. The results show that all samples exhibited relatively high relative density values, ranging from approximately 95% to 98%. The high relative density of the unreinforced aluminum sample indicates that the selected compaction and sintering parameters achieved effective densification. In addition, the relative density values remained largely low to moderate for BFS contents (%2–4), and some compositions exhibited values comparable to those of the unreinforced sample. This behavior suggests that BFS particles were successfully incorporated into the aluminum matrix without significantly impairing densification.

Nevertheless, a gradual decrease in relative density, accompanied by an increase in porosity, was observed as BFS content increased. This trend became more pronounced in composites containing 8–16 wt—% BFS. The increase in porosity can be attributed to enhanced particle–particle interactions, the formation of interfacial voids, and the partial restriction of densification mechanisms during sintering. Moreover, the reduction in matrix continuity and the tendency of reinforcement particles to agglomerate at high BFS contents may further promote pore formation.

Overall, the relative density values exceeding 95% demonstrate the effectiveness of the selected powder metallurgy processing parameters. However, the increase in porosity and the reduction in relative density observed at high BFS contents are consistent with the agglomeration tendencies identified in the optical microscopy analysis. They are expected to play a significant role in the subsequent hardness and wear behavior of the composites. These findings indicate that the addition of BFS does not significantly affect densification up to a certain reinforcement level. In contrast, excessive BFS content leads to a partial deterioration in the microstructural integrity of the composites.

3.2. Microstructural Analysis of Al–BFS Composite Materials

Figure 4 presents optical microscopy (OM) images at 100× magnification of the Al–BFS composite materials. These micrographs were used to evaluate the effect of BFS reinforcement content on the microstructural evolution of the composites.

Examination of the optical micrographs presented in Figure 4 reveals that BFS reinforcement significantly influenced the microstructure of the aluminum matrix. The unreinforced Al sample (S0) exhibited a relatively homogeneous microstructure with well-defined grain boundaries and high matrix continuity. With the addition of BFS, dark-colored regions corresponding to the reinforcement phase became visible within the matrix, and their volume fraction gradually increased as BFS content increased. At low reinforcement levels (0.125–1 wt.% BFS), the BFS particles appeared to be generally well distributed throughout the matrix, while matrix continuity was largely preserved, and no significant agglomeration tendency was observed. These observations indicate that the BFS particles were effectively surrounded by the aluminum matrix at low reinforcement contents, resulting in good microstructural integrity.

With increasing BFS content (2–4 wt.% BFS), the reinforcement phase became more pronounced within the microstructure, and localized particle accumulations began to appear as a result of the higher reinforcement concentration. In these samples, the interaction between the matrix and reinforcement phases appeared to increase, while the overall microstructural homogeneity was largely maintained. Nevertheless, the increase in reinforcement content made densification during sintering more challenging, resulting in the formation of small, isolated pores in certain regions of the microstructure.

A more pronounced change in the microstructure was observed in the composites containing high BFS contents (8–16 wt.% BFS). In particular, samples S7, S8, and S9 exhibited a substantial increase in the volume fraction of the dark reinforcement regions. In addition, the reinforcement particles tended to cluster in certain areas, leading to agglomerates and a partial reduction in matrix continuity. The decrease in the interparticle spacing at high reinforcement levels, together with insufficient diffusion during sintering, is believed to promote pore formation within the composite structure. The irregular voids and dark, clustered regions observed in the micrographs indicate that densification was adversely affected at high BFS contents. This interpretation is further supported by the experimental density and porosity results presented in the previous section.

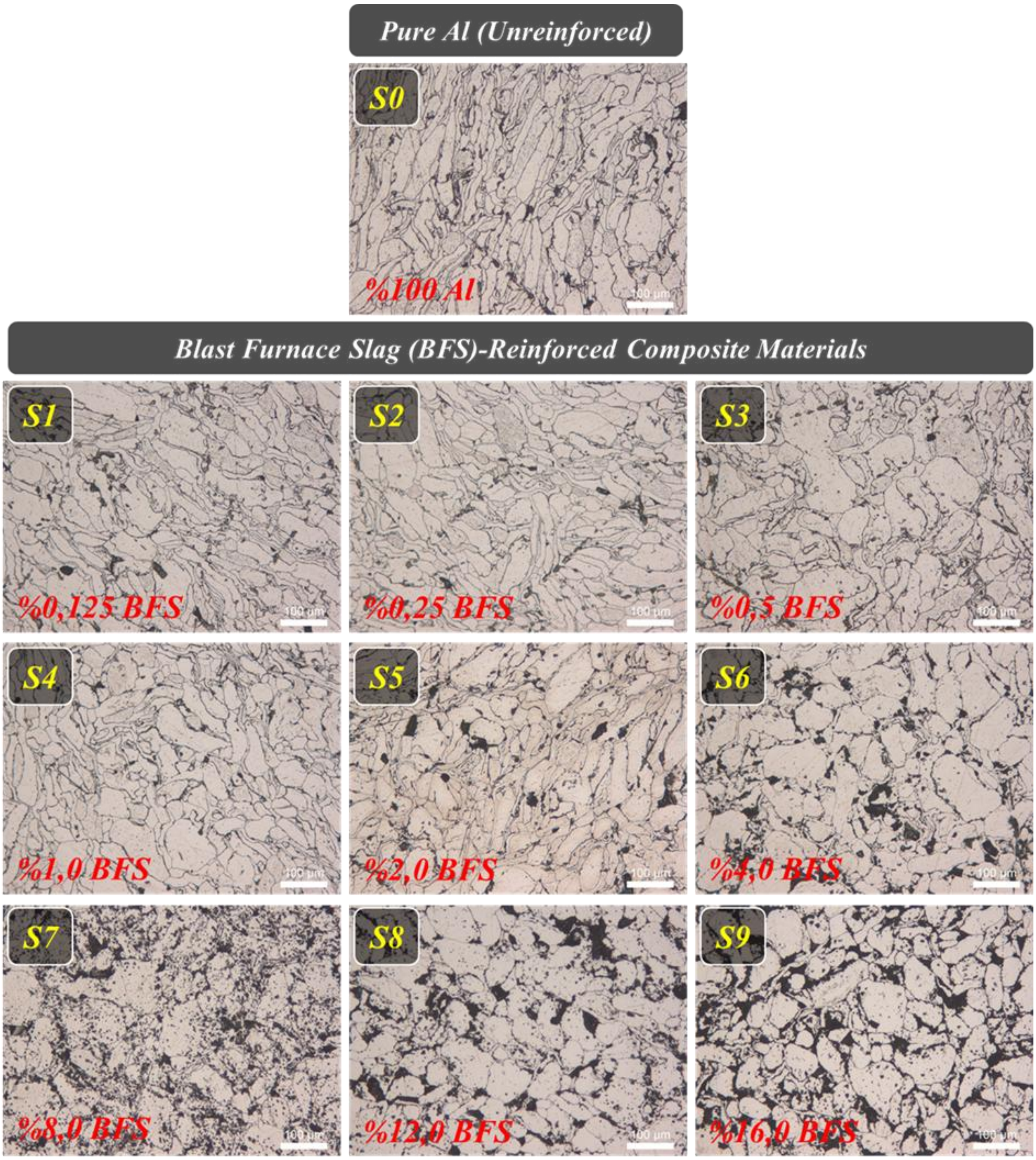

Figure 4. Optical microscopy (OM) images of the Al–BFS composite materials at 100× magnification.

Another noteworthy feature observed in the micrographs is a morphological change in the matrix structure as BFS content increases. The unreinforced aluminum sample exhibited relatively coarse and elongated grains, whereas the microstructure became progressively finer and more fragmented as the BFS content increased. This behavior may be attributed to the ability of BFS particles to partially restrict grain growth during sintering by acting as grain-boundary barriers. However, this interpretation should be supported by quantitative grain size measurements for definitive confirmation.

Overall, the optical microscopy results demonstrate that BFS reinforcement significantly influences the microstructural characteristics of the aluminum matrix composites. While low- and moderate-BFS contents resulted in a relatively homogeneous particle distribution and good microstructural integrity, higher reinforcement levels promoted particle agglomeration and pore formation. Consequently, BFS has the potential to enhance the performance of aluminum matrix composites; however, the beneficial effects may be limited at high reinforcement levels due to increased agglomeration and porosity. When considered together with the density, hardness, and wear results, the present findings indicate that not only the reinforcement content but also the homogeneity of the reinforcement particle distribution and the porosity level play critical roles in determining the overall performance of Al–BFS composites.

3.3. Hardness Measurements

The hardness behavior of the Al–BFS composites was investigated to evaluate the influence of BFS reinforcement on the materials' resistance to plastic deformation. Figure 5 illustrates the variation in macrohardness values with increasing BFS content.

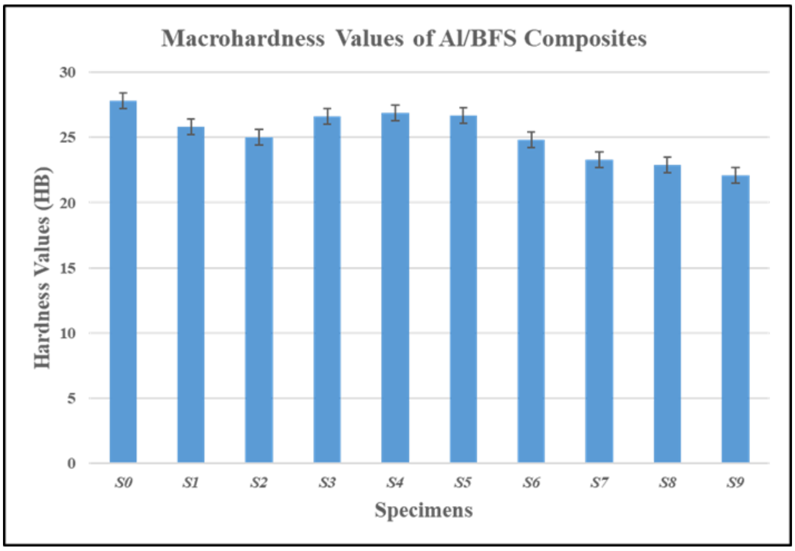

Figure 5. Variation of macrohardness values of Al–BFS composites with BFS reinforcement content.

Figure 5 shows the variation in the macrohardness values of the Al–BFS composites. The unreinforced aluminum sample (S0) exhibited the highest hardness value, approximately 27.8 HB. A slight decrease in hardness was observed at low BFS contents (0.125–0.5 wt.%). However, the hardness values increased again for the composites containing 1–4 wt.% BFS (S4–S6), reaching levels comparable to those of the unreinforced sample. In particular, the hardness values obtained for the composites containing 2 and 4 wt.% BFS can be attributed to the relatively homogeneous distribution of the reinforcement particles within the matrix and their contribution to the load-transfer mechanism. Moreover, the high relative density and low porosity values observed in these samples contributed to the preservation of hardness.

Nevertheless, a pronounced decrease in hardness was observed when the BFS content exceeded 8 wt.%. The lowest hardness value, approximately 22 HB, was recorded for the composite containing 16 wt.% BFS (S9). This reduction can primarily be attributed to the decrease in relative density and the increase in porosity identified in the density measurements, as well as the microstructural changes observed in the optical micrographs. In particular, the tendency of reinforcement particles to agglomerate, the reduction in matrix continuity, and the increase in pore content at high BFS levels promoted stress concentration under the applied load, thereby reducing resistance to plastic deformation. Since increased porosity reduces the effective load-bearing cross-sectional area in powder metallurgy composites, it directly contributes to the deterioration of hardness.

Optical microscopy observations revealed a relatively homogeneous microstructure at BFS contents of 2–4 wt.%, whereas particle agglomeration and irregular pore formation became increasingly evident at higher reinforcement levels. These findings are consistent with the increase in porosity determined from the density measurements and support the observed reduction in hardness. Although BFS is a ceramic-rich reinforcement containing hard oxide phases that would be expected to improve hardness, the potential strengthening effect was counteracted by the formation of microstructural defects and the deterioration of densification behavior at BFS contents exceeding 4 wt.%. Consequently, the adverse effects of porosity and particle agglomeration became dominant at higher reinforcement levels, leading to a reduction in the overall mechanical performance of the composites.

Overall, the results indicate that the effect of BFS reinforcement on hardness is not linear. The hardness behavior of the composites is governed not only by the reinforcement content but also by the degree of densification, porosity level, and distribution homogeneity of the reinforcement particles within the matrix. While the relatively homogeneous microstructure and high relative density values obtained at BFS contents of 2–4 wt.% contributed to maintaining hardness performance, increased porosity and particle agglomeration at BFS contents above 4 wt.% resulted in a significant reduction in hardness. Considering the combined effects of densification behavior, microstructural integrity, and hardness performance, BFS contents of 2–4 wt.% provided the most favorable mechanical performance among the investigated composites.

3.4. Wear Tests

Pin-on-disk wear tests were conducted to evaluate the tribological behavior of the Al–BFS composite materials. The wear performance of the composites was assessed using weight-loss measurements obtained after testing, and the corresponding results are presented in Figure 6.

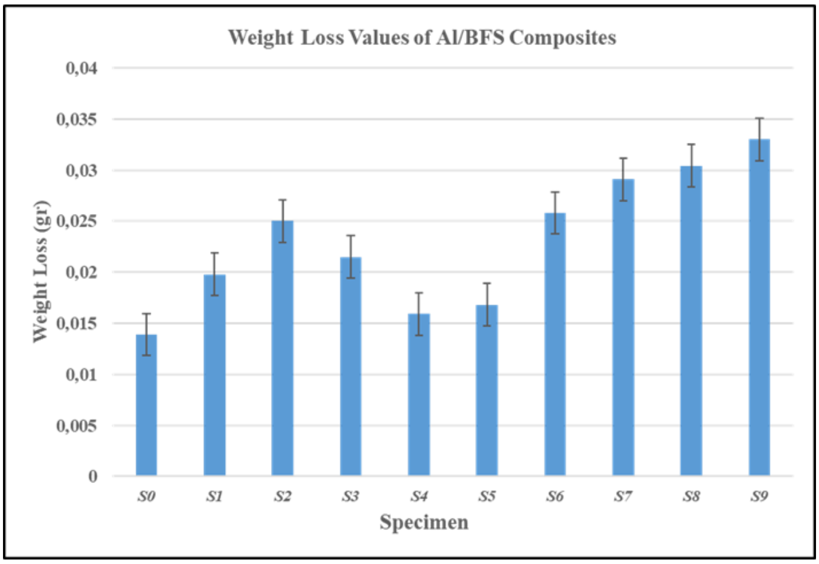

Figure 6. Weight loss values of the Al–BFS composite materials after wear testing.

Figure 6 illustrates the wear behavior of the Al–BFS composites in terms of weight loss after wear testing. The results indicate that the BFS reinforcement content significantly influenced the wear performance of the composites. The lowest weight loss, approximately 0.014 g, was obtained for the unreinforced aluminum sample (S0). In general, weight loss increased with increasing BFS content, indicating a gradual deterioration in wear resistance. This trend became particularly pronounced in the composites containing 8–16 wt.% BFS, with the highest weight loss value of approximately 0.033 g recorded for the S9 sample containing 16 wt.% BFS.

The wear results are more meaningful when evaluated alongside the density and porosity measurements. As discussed in the previous sections, increasing BFS content resulted in lower experimental and relative density values, accompanied by a noticeable increase in porosity. In powder metallurgy composites, porosity reduces the effective load-bearing area and facilitates material removal from the surface during sliding contact. Therefore, the increase in wear loss observed at high BFS contents can be largely attributed to the increased porosity within the composite structure.

The optical microscopy observations further support this interpretation. At low reinforcement levels, the BFS particles were relatively homogeneously distributed throughout the matrix. In contrast, higher reinforcement contents resulted in particle agglomeration and the formation of irregular pores. In particular, the agglomerated regions observed in samples S7, S8, and S9 may have acted as stress concentration sites during wear, thereby accelerating particle pull-out and surface damage. As a result, more material was removed from the worn surface, leading to higher weight-loss values.

A similar trend was observed when the wear behavior was compared with the hardness results. While the hardness values of the composites containing 2–4 wt.% BFS remained comparable to those of the unreinforced aluminum sample, a significant reduction in hardness was observed at higher reinforcement levels (≥8 wt.% BFS). Since wear resistance is generally correlated with hardness, the reduction in hardness contributed to the increased wear loss. Furthermore, the increased porosity and particle agglomeration observed at higher BFS contents promoted microstructural heterogeneity, thereby accelerating material removal during sliding. Notably, samples S7–S9, which exhibited the lowest hardness values, also showed the highest weight loss values, indicating a strong relationship between hardness degradation and wear performance.

Overall, the results demonstrate that the effect of BFS reinforcement on wear behavior is not governed solely by reinforcement content. Instead, the tribological performance of the composites is strongly influenced by microstructural homogeneity, porosity level, and densification behavior. The composites containing 2–4 wt.% BFS exhibited the most favorable wear performance among the reinforced samples, whereas BFS contents of 8 wt.% and above adversely affected wear resistance because of increased porosity, particle agglomeration, and reduced hardness. Consequently, increasing the BFS content beyond 4 wt.% did not improve the tribological performance of the Al–BFS composites; rather, it led to a progressive deterioration in wear resistance despite the ceramic-rich nature of the reinforcement phase.

4. Conclusion

In this study, pure aluminum matrix composites reinforced with varying amounts of blast-furnace slag (BFS) were successfully fabricated via powder metallurgy, and the effects of BFS addition on density, microstructure, hardness, and wear behavior were systematically investigated. The results demonstrated that BFS reinforcement significantly influences the microstructural, mechanical, and tribological properties of aluminum matrix composites, and that these effects strongly depend on the reinforcement content.

Density measurements revealed that the addition of BFS had only a minor influence on the theoretical density of the composites. However, increasing the BFS content resulted in lower experimental and relative density values and higher porosity levels. Although all composites exhibited relative densities above 95%, the increase in porosity observed at BFS contents of 8–16 wt.% indicated a gradual deterioration in densification behavior. Optical microscopy observations supported these findings, showing relatively homogeneous microstructures at BFS contents of 2–4 wt.%. In contrast, particle agglomeration, irregular pore formation, and reduced matrix continuity became increasingly evident at BFS contents of 8 wt.% and above.

The mechanical and tribological properties were found to be closely related to these microstructural changes. While the hardness values of the composites containing 2–4 wt.% BFS remained comparable to those of the unreinforced aluminum sample, a significant reduction in hardness was observed at BFS contents of 8 wt.% and above due to increased porosity and particle agglomeration. Similarly, wear tests revealed a progressive increase in weight loss with increasing BFS content. The deterioration in wear resistance was associated with increased porosity, reduced matrix continuity, and microstructural heterogeneity, all of which contributed to the observed reduction in hardness and accelerated material removal during sliding.

Overall, the results indicate that the performance of Al–BFS composites is governed not only by the amount of reinforcement but also by the degree of densification, the porosity level, and the homogeneity of the distribution of reinforcement particles within the matrix. The findings demonstrate that blast furnace slag can be used as a low-cost, environmentally sustainable reinforcement material in aluminum matrix composites. However, excessive BFS additions promote microstructural defects that adversely affect the mechanical and tribological performance of the composites. Considering all experimental results together, optimum performance was achieved at low to moderate BFS contents. In contrast, high reinforcement levels should be avoided due to their detrimental effects on densification, hardness, and wear resistance.

Acknowledgment

This study was supported by the Scientific and Technological Research Council of Türkiye (TÜBİTAK) through the 2209-A University Students Research Projects Support Program. The authors gratefully acknowledge the support provided by TÜBİTAK BİDEB (Scientist Support Programs Presidency).

Conflict of Interest

The authors declare that they have no conflict of interest.

Disclosure of Generative AI Use

An AI tool was used in language editing and grammar refinement during the preparation of this article.

References

Abdizadeh, H., Ebrahimifard, R., & Baghchesara, M. A. (2014). Investigation of microstructure and mechanical properties of nano MgO reinforced Al composites manufactured by stir casting and powder metallurgy methods: A comparative study. *Composites Part B: Engineering*, *56*, 217-221. https://doi.org/10.1016/j.compositesb.2013.08.023

Babu, K. G., & Kumar, V. S. R. (2000). Efficiency of GGBS in concrete. *Cement and Concrete Research*, *30*(7), 1031-1036. https://doi.org/10.1016/S0008-8846(00)00271-4

Bilim, C., & Atiş, C. D. (2011). Öğütülmüş granüle yüksek fırın cürufu içeren harçların aşınma ve mukavemet özellikleri. *Politeknik Dergisi*, *14*(2), 101-107. (In Turkish)

Binici, H., Görür, E. B., & Durgun, M. Y. (2016). Yüksek fırın cürufu ve bazaltik pomza katkılı betonların mekanik aşınması ve su geçirimliliği. *Yapı Teknolojileri Elektronik Dergisi*, *6*(1), 1-10. (In Turkish)

Chen, R., & Zhang, G. (1993). Casting defects and properties of cast A356 aluminium alloy reinforced with SiC particles. *Composites Science and Technology*, *47*(1), 51-56. https://doi.org/10.1016/0266-3538(93)90095-X

Chintada, S., Dora, S. P., Kare, D., & Pujari, S. R. (2022). Powder metallurgy versus casting: Damping behavior of pure aluminum. *Journal of Materials Engineering and Performance*, *31*(11), 9122-9128. https://doi.org/10.1007/s11665-022-06886-2

Dorum, A., Koçak, Y., Yılmaz, B., & Uçar, A. (2009). Yüksek fırın cürufunun çimento yüzey ve hidratasyona etkileri. *Journal of Science and Technology of Dumlupınar University*, (019), 47-58. (In Turkish)

Douglas, E., & Brandstetr, J. (1990). A preliminary study on the alkali activation of ground granulated blast-furnace slag. *Cement and Concrete Research*, *20*(5), 746-756. https://doi.org/10.1016/0008-8846(90)90008-L

Erdoğan, T. Y. (1995). *Öğütülmüş granüle yüksek fırın cürufu ve kullanımı*. TMMOB İnşaat Mühendisleri Odası Bildiriler Kitabı, Endüstriyel Atıkların İnşaat Sektöründe Kullanılması Sempozyumu. (In Turkish)

Erdoğdu, Ş., & Kurbetçi, Ş. (2003). Betonun performansına sağladıkları etkinlik açısından kimyasal ve mineral katkı maddeleri. *Türkiye Mühendislik Haberleri*, *426*(4), 115-120. (In Turkish)

Gräbner, M., Wiche, H., Treutler, K., & Wesling, V. (2022). Micromagnetic properties of powder metallurgically produced Al composites as a fundamental study for additive manufacturing. *Applied Sciences*, *12*(13), 6695. https://doi.org/10.3390/app12136695

Hull, D. (1998). *An introduction to composite materials*. Cambridge University Press

Kok, M. (2005). Production and mechanical properties of Al2O3 particle-reinforced 2024 aluminium alloy composites. *Journal of Materials Processing Technology*, *161*(3), 381-387. https://doi.org/10.1016/j.jmatprotec.2004.07.068

Kumar, D. R., Loganathan, C., & Narayanasamy, R. (2011). Effect of glass in aluminum matrix on workability and strain hardening behavior of powder metallurgy composite. *Materials & Design*, *32*(4), 2413-2422. https://doi.org/10.1016/j.matdes.2010.12.008

Malolepszy, J., & Petri, M. (1986). *High strength slag alkaline binders*. 8th International Congress on the Chemistry of Cement. Rio de Janeiro.

Nayak, K. C., Rane, K. K., Date, P. P., & Srivatsan, T. S. (2022). Synthesis of an aluminum alloy metal matrix composite using powder metallurgy: Role of sintering parameters. *Applied Sciences*, *12*(17), 8843. https://doi.org/10.3390/app12178843

Özer, M., Kaplan, Y., Özer, A., & Aksoz, S. (2024). Influence of different sintering techniques on the wear properties of Al-15Si-2.5 Cu-0.5 Mg/B4C composites. *Science of Sintering*, *56*(3), 269-283. https://doi.org/10.2298/SOS231003060O

Özkan, Ö. (2007). Atık cam ve yüksek fırın cürufu katkılı harçların özellikleri. *Gazi Üniversitesi Mühendislik Mimarlık Fakültesi Dergisi*, *22*(1). (In Turkish)

Şanlı, A. (2017). *Al 6061 matrisli SiC, Al2O3 ve yüksek fırın cürufu takviyeli hibrit kompozitlerin yorulma davranışlarının incelenmesi* (Master's thesis, Bartın University). (In Turkish)

Şap, S., Turgut, A., & Uzun, M. (2021a). Investigation of microstructure and mechanical properties of Cu/Ti–B–SiC_p hybrid composites. *Ceramics International*, *47*(21), 29919-29929. https://doi.org/10.1016/j.ceramint.2021.07.165

Şap, S., Uzun, M., Usca, Ü. A., Pimenov, D. Y., Giasin, K., & Wojciechowski, S. (2021b). Investigation on microstructure, mechanical, and tribological performance of Cu base hybrid composite materials. *Journal of Materials Research and Technology*, *15*, 6990-7003. https://doi.org/10.1016/j.jmrt.2021.11.114

Saran, A. G. (2007). *Öğütülmüş granüle yüksek fırın cürufunun betonun durabilite özelliklerine etkisi* (Master's thesis, İstanbul Technical University). (In Turkish)

Şenel, M. C. (2020). Toz metalürjisi yöntemiyle üretilen saf Al ve Al-B4C, Al-Al2O3 kompozitlerin mekanik ve mikroyapı özelliklerinin karşılaştırılması. *Gümüşhane Üniversitesi Fen Bilimleri Dergisi*, *10*(3), 783-795. https://doi.org/10.17714/gumusfenbil.689359 (In Turkish)

Shi, C. J., & Day, R. L. (1992). *Comparison of the microstructure and performance of alkali-slag and Portland cement pastes*. 9 th International Congress on the Chemistry of Cement. New Delhi.

Tokyay, M., & Erdoğdu, K. (2002). *Cüruflar ve cüruflu çimentolar*. TÇMB. (In Turkish)

Usca, Ü. A., Şap, S., Uzun, M., Giasin, K., & Pimenov, D. Y. (2022). Evaluation of mechanical and tribological aspect of self-lubricating Cu-6Gr composites reinforced with SiC–WC hybrid particles. *Nanomaterials*, *12*(13), 2154. https://doi.org/10.3390/nano12132154

Usca, Ü. A., Uzun, M., Kuntoğlu, M., Şap, S., Giasin, K., & Pimenov, D. Y. (2021). Tribological aspects, optimization and analysis of Cu-B-CrC composites fabricated by powder metallurgy. *Materials*, *14*(15), 4217. https://doi.org/10.3390/ma14154217

Yalçın, H., & Gürü, M. (2006). *Çimento ve beton*. Palme Yayıncılık. (In Turkish)